JACS
JOURNAL OF THE AMERICAN CHEMICAL SOCIETY
pubs.acs.org/JACS
Article

Cathode−Anode Synergy Electrosynthesis of Propanamide via a Bipolar C−N Coupling Reaction

Ming-Hao Guan, Hao-Nan Xu, Jin Liu, Xiao-Ya Zhou, Tao Wu,* and An-Hui Lu*

Cite This: J. Am. Chem. Soc. 2025, 147, 16301−16308
Read Online

ACCESS | Metrics & More | Article Recommendations | Supporting Information

ABSTRACT: Propanamide is a crucial synthetic intermediate in pharmaceuticals for the preparation of antibacterial and anticancer drugs. Conventional synthesis of propanamide involves the reaction of carboxylic acid derivatives with amines, which requires harsh reaction conditions, leading to an unfavorable environmental footprint. Here, we present a cathode−anode synergistic electrochemical strategy to transform nitrate and n-propanol into propanamide under ambient conditions, where both the cathode catalyst Co_3O_4/SiC and the anode catalyst Ti contribute distinctively to the electrochemical process. The CH_3CH_2CHO produced at the Ti anode can diffuse and react with the adsorbed intermediate *NH_2OH on the surface of the cathode catalyst to form propanamide. The synergistic reactions at both electrodes collectively enhance the efficiency of the propanamide synthesis. This design enables efficient propanamide production in a flow cell at the gram scale with a remarkable yield of 986.13 μmol/(cm^2·h) at current densities of up to 650 mA/cm^2. Our reports present a new option for environmentally friendly C−N bond synthesis, and the insights can be useful for the electrosynthesis of a wider scope of amides.

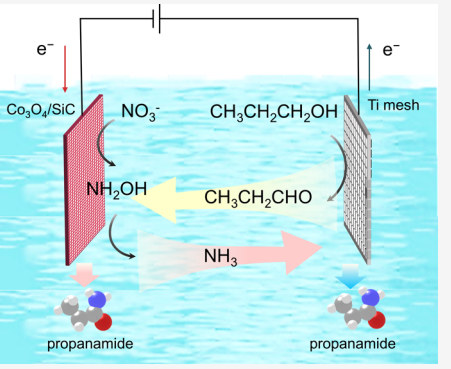

INTRODUCTION

Amides are one of the most crucial organic chemicals and are extensively utilized across various industries, such as polymers, pharmaceuticals, dyestuffs, agrochemicals, and emulsifiers.[1−3] Propanamide, in particular, serves as a vital synthetic intermediate in pharmaceutical applications, with its derivatives contributing to the development of antibacterial and anticancer agents.[4,5] Nevertheless, conventional industrial methods for amide synthesis predominantly involve the reaction of carboxylic acid derivatives with amines, necessitating additional synthetic steps that are often performed at elevated temperatures.[6,7] This reliance on carboxylic acid derivatives not only complicates the synthesis but also increases energy consumption, underscoring the necessity for more efficient and sustainable alternatives in the production of amides. Moreover, carboxylic acid derivatives require additional synthetic steps, often conducted at high temperatures with the intervention of coupling agents, such as carbodiimides, uronium/phosphonium salts, or benzotriazoles (Figure S1).[8] These reactions not only suffered from poor atomic efficiency and use of expensive reagents, but also caused environmental concerns.[9−11] Consequently, sustainable green amide synthesis is critically important and was recognized as one of the top ten research areas in chemistry by the ACS Green Chemistry Institute Pharmaceutical Roundtable (GCIPR).[12]

An electrochemical method for the synthesis of amides holds great promise as an environmentally friendly alternative.[13−17] For instance, the electrosynthesis of methylamine, acetamide, and formamide has been successfully demonstrated utilizing CO_2/CO as the carbon source.[2,18] These notable advancements have predominantly concentrated on electrochemical reduction processes for C−N bond formation. However, the sluggish anodic oxygen evolution reaction (OER) necessitates the application of high potentials.[19] Meanwhile, the complex reaction pathways of cathodic electrochemical CO_2/CO reduction produce only a small amount of active species capable of combining with nitrogen sources for C−N coupling, greatly limiting the Faradaic efficiency (FE) of amide synthesis (usually <40%).[20,21] Moreover, the active carbon species generated from CO_2/CO reduction predominantly consist of C_1 and C_2 species, making it challenging to produce higher-carbon-number and more complex functionalized amide products. Thus, the investigation of alternative electrooxidation processes using readily available carbon- and nitrogen-containing feedstocks to synthesize high-valued amide under ambient conditions is highly desirable.

Herein, a new and sustainable cathode-anode synergistic electrocatalytic system is reported to convert nitrate ions (NO_3^-) and n-propanol ($CH_3CH_2CH_2OH$) into propanamide

Received: January 29, 2025
Revised: April 23, 2025
Accepted: April 23, 2025
Published: May 2, 2025

https://doi.org/10.1021/jacs.5c01744
J. Am. Chem. Soc. 2025, 147, 16301−16308

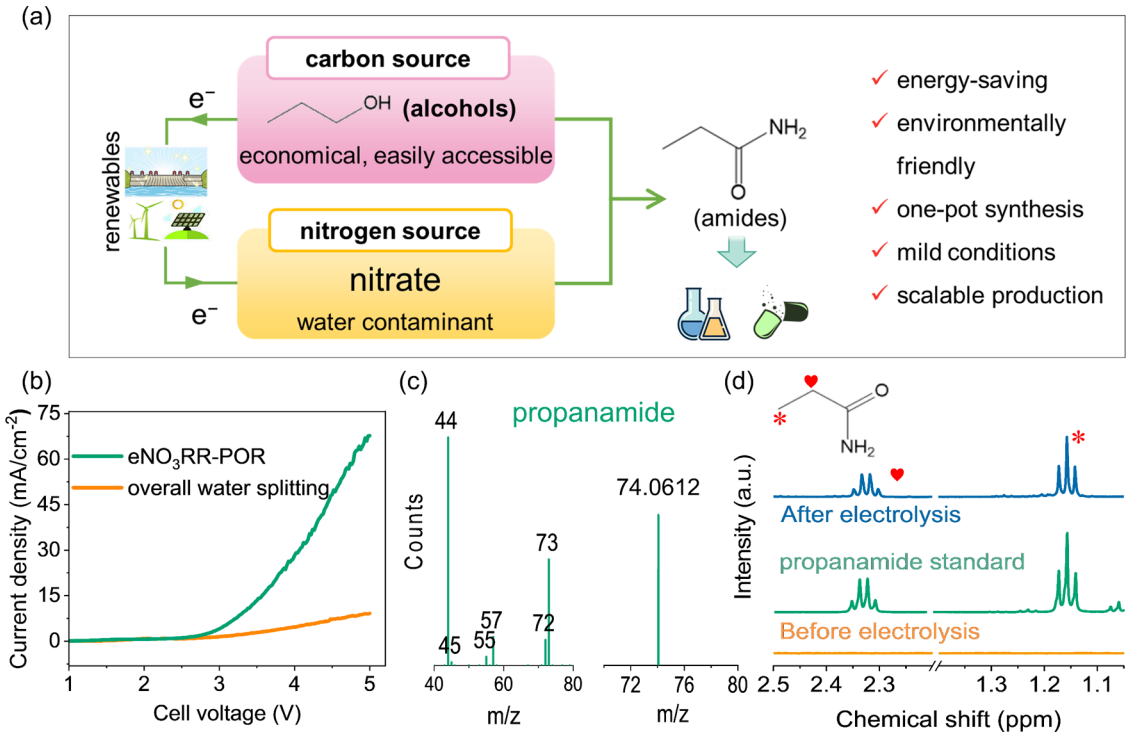

Figure 1. Illustration of the route for yielding propanamide by the bipolar C−N coupling. (a) Schematic diagram of the electrochemical cathode-anode coupling strategy to produce propanamide using NO_3^- and n-propanol. (b) LSV curves of eNO_3RR-POR and eHER-OER, (c) GC-MS, HPLC-MS, and (d) ^{1}H NMR detection of propanamide.

under ambient conditions (Figure 1a). Nitrate reduction occurs at the cathode, while n-propanol oxidation takes place at the anode with Co_3O_4/SiC and Ti serving as the cathode and anode catalysts, respectively. By substituting the high-energy-consuming oxygen evolution reaction with alcohol oxidation, it can maximize the utilization of the anode reaction, thereby improving energy efficiency.[22] The cathodic FE for propanamide could reach 74.52% in the three-electrode test. Moreover, this design enables efficient propanamide production in a flow cell at the gram scale, with a remarkable yield of 986.13 μmol/(cm^2·h) at current densities of up to 650 mA/cm^2. Combined with the comparative experiment and density functional theory (DFT) calculations, we find that the chemicals generated at both electrodes are capable of diffusing to their respective counter electrodes and undergoing further reactions with the adsorbed intermediates on the surface of the catalysts, consequently enhancing the efficiency of propanamide synthesis. Notably, technical economic analysis results demonstrate that this reaction holds great potential for industrial applications, as it offers a high-yield synthetic route.

RESULTS AND DISCUSSION

Bipolar Electrosynthesis of Propanamide by C−N Coupling. Propanamide electrosynthesis by the coupling reaction of the anode and cathode from n-propanol and NO_3^- is performed in a single cell, unless otherwise specified. The cathode catalyst used for the nitrate reduction reaction (NO_3RR) was Co_3O_4/SiC, which demonstrated remarkable activity in converting nitrate to ammonia in our previous study.[23] Figures S2a and S3 present the characterization analysis of Co_3O_4/SiC, revealing that its structure comprises Co_3O_4 and SiC phases. Several metal materials, including Cu, Ni, Ti, Pt, and Pt/Ti, have been screened as the anode for propanamide synthesis (Figure S4). After 2 h of electrolysis tests, Cu and Ni exhibited almost no yield for propanamide. This may be due to metal dissolution instead of alcohol oxidation occurring at the anode potential, as indicated by the experimental observation that the electrolyte changes from a colorless and transparent solution to color and turbidity associated with metal ions. The inert oxide film formed on the Ti in air or water protects it from further oxidation, thereby enhancing its performance (Figure S5). Ti and Pt demonstrated comparable activity in propanamide synthesis; nevertheless, considering the cost-effectiveness of the catalysts, Ti was selected as the anode catalyst. The XRD pattern and SEM images of the Ti mesh catalyst are presented in Figures S2b and S6.

Figure 1b shows the linear sweep voltammetry (LSV) polarization curves for traditional water electrolysis (eHER-OER) and the coupling reaction (eNO_3RR-POR) of cathodic nitrate reduction (NO_3RR) and anodic n-propanol oxidation (POR). With the addition of NO_3^- and n-propanol to the cathode and anode feed, the onset potential was reduced and the current densities for the eNO_3RR-POR system were significantly higher than those for the eHER-OER system at voltage above 2.5 V, indicating that the synergy coupling system has higher reaction activity than water electrolysis. Furthermore, the products in the cell configuration were identified through gas chromatography−mass spectrometry (GC−MS), high-performance liquid chromatography−mass spectrometry (HPLC−MS), and ^{1}H-nuclear magnetic resonance (^{1}H NMR) spectroscopy, as shown in Figure 1c,d, confirming the production of propanamide.

To clarify the processes of the cathode and anode reactions, the individual reactions were investigated separately using a three-electrode system. The cathode hosts a nitrate reduction

https://doi.org/10.1021/jacs.5c01744
J. Am. Chem. Soc. 2025, 147, 16301−16308

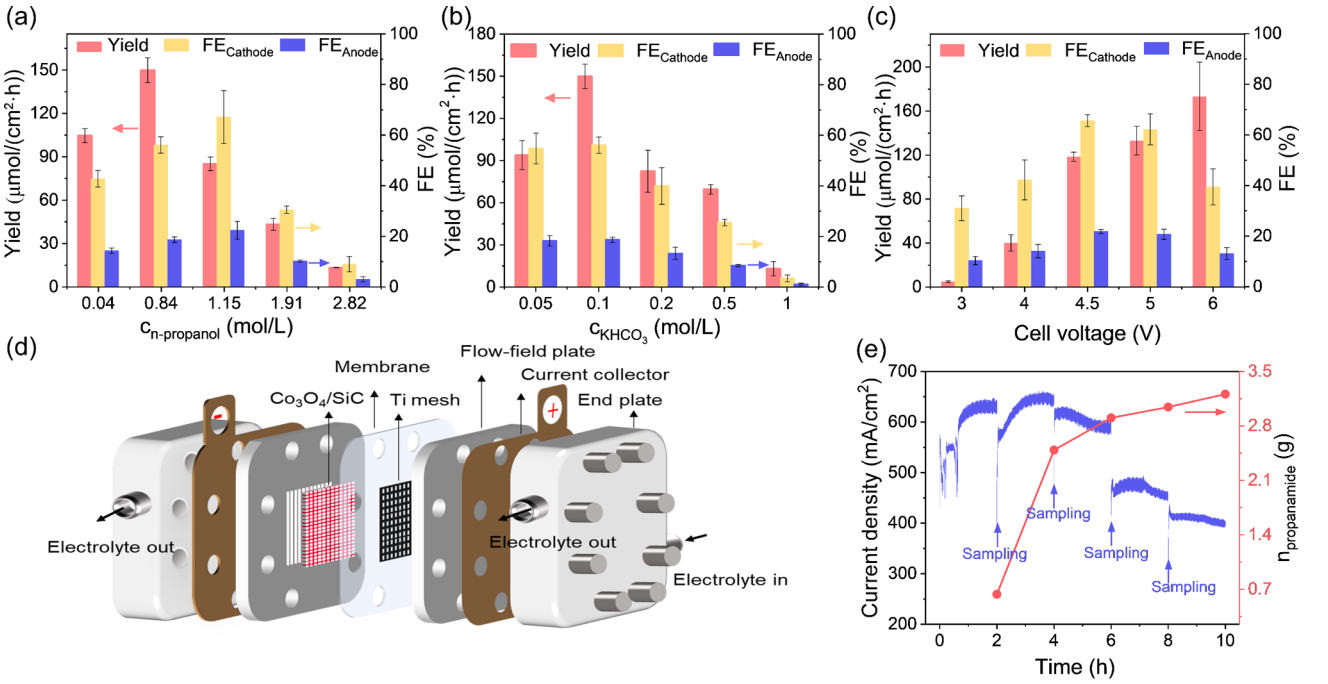

Figure 2. Catalytic performance of bipolarly producing propanamide. The yield and FE of propanamide in various (a) concentrations of n-propanol, (b) concentrations of $KHCO_3$, and (c) cell voltages. (d) Schematic of the eNO_3RR-POR using a membrane electrode flow cell with a Nafion 117 membrane. (e) The current density and accumulated propanamide in the flow cell measurement.

reaction for ammonia synthesis. The nitrate reaction of the cathode showed good activity in both neutral and alkaline electrolytes (Figure S7). In a 1 M KOH alkaline solution, the NH_3 yield can reach 0.75 mmol/(cm^2·h) with a FE exceeding 80% at −0.8 V vs RHE. The NH_3 yield can achieve 0.90 mmol/(cm^2·h) with a FE of 95% in a 1 M Na_2SO_4 solution, at −0.9 V vs RHE.

The anode was used to hold the alcohol oxidation reaction. Figure S8a presents the LSV test results conducted in 0.1 M $KHCO_3$ and 1 M $NaNO_3$ electrolyte, with and without n-propanol. The oxidation current in the n-propanol system is substantially greater than that in the pure water system. However, at high potential ranges, the oxidation currents for both systems converge to nearly the same level. This observation suggests that the oxidation of n-propanol predominantly occurs during the initial stage, while competition from the OER intensifies as the potential increases. Simultaneously, the Tafel slope was determined based on the LSV data for assessing the reaction kinetics, as illustrated in Figure S8b. The Ti mesh had a significantly lower Tafel slope of 70.07 mV/dec for n-propanol oxidation compared to that of the OER (97.88 mV/dec), indicating enhanced catalytic kinetics at the anode. Furthermore, electrochemical impedance spectroscopy (EIS) conducted at 1.7 V vs RHE across frequencies from 10^6 to 0.1 Hz indicated that the charge transfer resistance for the n-propanol oxidation reaction was significantly smaller than that of the OER (Figure S8c).

Catalytic Performance of C−N Coupling to Propanamide. Subsequently, we integrated the anode reaction with the cathodic nitrate reduction reaction to synthesize propanamide using the three-electrode system without a separator, wherein the Co_3O_4/SiC served as the working electrode, titanium mesh functioned as the counter electrode, and the Ag/AgCl electrode was employed as the reference electrode. The results (Table S1) demonstrated that propanamide was produced under neutral and weakly alkaline conditions, while only propionic acid was formed under strongly alkaline conditions. This observation indicates that the high concentration of OH^- ions promotes the further oxidation of the anodic products, leading to the formation of propionic acid. As shown in Figure 2a, the yield and FE of propanamide exhibited a volcano-shaped curve as the concentration of n-propanol increased. At a concentration of 0.84 mol/L of n-propanol, the maximum yield of propanamide is 143.77 μmol/(cm^2·h) which is normalized to catalyst mass of 79.87 mmol/(g_{cat}·h), while at a concentration of 1.15 mol/L of n-propanol, the FE of propanamide at the cathode reaches 74.52%. This phenomenon, derived from the initial rise in n-propanol concentration, facilitated the mass transfer of the anode reaction, leading to an increased formation of propionaldehyde, an intermediate product of n-propanol oxidation. The insufficient consumption rate, however, led to the further oxidation of excess n-propanol to propionic acid upon further introduction of n-propanol. Moreover, the impact of the electrolyte concentration on the reaction has also been investigated (Figure 2b). A high concentration of HCO_3^- undergoes hydrolysis to generate OH^-, which will also accelerate the formation of propionic acid. After the above-mentioned investigation, a $KHCO_3$ concentration of 0.1 M is deemed most suitable for the synthesis of propanamide.

We next used a two-electrode system with a Ti mesh as the anode and Co_3O_4/SiC as the cathode to explore the optimal reaction potential for subsequent flow cell experiments. Consistently, the system was operated in the absence of a separator, and the corresponding I−t curves are depicted in Figure S9. With the increase in cell voltage, the yield of propanamide continues to rise; however, the FE exhibits a volcano-shaped curve, reaching the maximum value of 67.23% (cathode side) at 4.5 V (Figure 2c). This phenomenon is attributed to the simultaneous increase in anode and cathode

https://doi.org/10.1021/jacs.5c01744
J. Am. Chem. Soc. 2025, 147, 16301−16308

Table 1. Different Control Experiments[a]

entry	carbon source	nitrogen source	cell type	electricity or not	propanamide
1	n-propanol	NO_3^-	Single cell	√	√
2		NO_3^-	Single cell	√	×
3	n-propanol		Single cell	√	×
4	n-propanol	NO_3^-	Single cell	×	×
5	n-propanol	NO_3^-	H type cell	√	×
6	propionaldehyde	NO_3^-	H type cell-cathode	√	√
7	propionic acid	NO_3^-	H type cell-cathode	√	×
8	n-propanol	NH_3	H type cell-anode	√	√
9	n-propanol	NH_2OH	H type cell-anode	√	×
10	n-propanol	NO_3^-	H type cell mixing cathode and anode electrolytes after electrolysis		×

[a]The presence of symbol √ indicates the formation of propanamide, while symbol × suggests the absence of propanamide.

overpotentials due to elevated cell voltage. Consequently, n-propanol at the anode undergoes overoxidation, leading to the cleavage of C−C bonds and the production of formic acid. Additionally, higher overpotentials promote OERs at the anode while intensifying competition with hydrogen evolution reactions at the cathode. The liquid C-containing products were analyzed by GC-MS as shown in Figure S10, which included propionaldehyde, propionaldehyde oxime, propionic acid, n-propyl propionate, and propionitrile. Moreover, a small amount of the excessive oxidation product CO_2 was detected as shown in Table S2. The products are displayed in Figure S11 and Table S3.

To minimize ohmic resistance between electrodes, a membrane electrode assembly flow reactor was further constructed for converting NO_3^- into ammonia paired with n-propanol oxidization to produce propanamide (Figure 2d). 0.1 M $KHCO_3$ and 1 M $NaNO_3$ with n-propanol were used as both cathode and anode electrolytes and circulated within a common tank. Chronoamperometry tests were conducted using this experimental setup, and the results are displayed in Table S4. To our surprise, the membrane electrode test achieved a current density of up to 650 mA/cm^2 and a propanamide yield of 986.13 μmol/(cm^2·h) that normalized to catalyst mass is 547.85 mmol/(g_{cat}·h), both of which are about ten times higher than those obtained from the single-cell test. The superior current density and propanamide yield make it one of the advanced electrocatalytic C−N coupling routes and show great potential for industrial application. Compared to the existing literature, the performance advantage of our work is evident (Table S5). Under a cell voltage of 5 V, the conversion of n-propanol gradually increased (Figure S12), ultimately reaching 83.5%, while the current density decreased originating from reactant consumption during the 10-h reaction (Figure 2e). The selectivity of propanamide is 20% after the test. The obtained propanamide was detected by infrared spectroscopy and NMR as illustrated in Figures S13 and S14. Additionally, we conducted a stability test, during which the production of propanamide initially showed a slight decline and gradual stabilization over a 32 h cycle (Figure S15). During the first cycle, the cathode Co_3O_4 was partially reduced under high-current density conditions, which caused a decrease in NO_3RR activity and subsequently reduced the Faraday efficiency of propanamide. However, the majority of Co_3O_4 does not undergo further reduction, owing to its strong interaction with the SiC carrier. XPS analysis in Figure S16 revealed that the proportion of trivalent cobalt decreased from 40 to 29% after the first cycle but remained at ∼27% after eight cycles, suggesting that the catalyst's surface properties stabilized after initial reduction. Moreover, the anode titanium mesh catalyst showed no changes in both XRD and Raman spectroscopy analyses post-test (Figure S17), indicating its excellent stability.

Reaction Mechanism of Cathode−Anode Synergy Electrosynthesizing Propanamide. The high efficiency of the bipolar electrocatalytic synthesis of propanamide prompted us to further investigate its underlying mechanism. A series of control experiments were conducted and are presented in Figure S18, along with entries 1−4 in Table 1.

The absence of propanamide formation upon removal of one of the applied potential, n-propanol, or NO_3^- indicates that the generated propanamide is derived from the simultaneous electrocatalytic reduction of NO_3^- and oxidation of n-propanol. When the cathode and anode reactions were separated by the nafion membrane, which selectively transports protons in an H-type cell (entry 5 in Table 1), no propanamide was detected, indicating a requirement for further coupling reactions between the cathode and the anode intermediate products. The formation of propanamide was observed when propionaldehyde was used as the carbon source on the split cathode side, whereas no propanamide was formed when propionic acid was fed (entries 6 and 7 in Table 1). These results suggest that propionaldehyde, rather than propionic acid, played the intermediate species role joint on the cathode side.

Similarly, the reaction on the anode side of the split cell was also investigated in entries 8 and 9. When NH_3 and NH_2OH were utilized as the nitrogen sources, only NH_3 generated propanamide, indicating that reactant NH_3 was involved in the synthesis of propanamide on the anode side. In entry 10, the electrolytic reaction is initially conducted in a separate H-type cell. Subsequently, the anode and cathode electrolytes are mixed but no propanamide product, indicating that the coupling reaction between the anode and cathode is not a direct solution-phase chemical reaction of the individual products from each electrode but rather an electrocatalyst surface reaction under a localized electric field involving the coupling of intermediates.

To further gain insights into the reaction route and mechanism of activity enhancement, attenuated total reflection in situ Fourier transform infrared (ATR-FTIR) spectrometer analysis and a thin-layer in situ FTIR technique are employed to track intermediates.[24] A three-electrode system was employed for in situ FTIR testing, wherein Co_3O_4/SiC served as the working electrode and titanium mesh, the Ag/AgCl

https://doi.org/10.1021/jacs.5c01744
J. Am. Chem. Soc. 2025, 147, 16301−16308

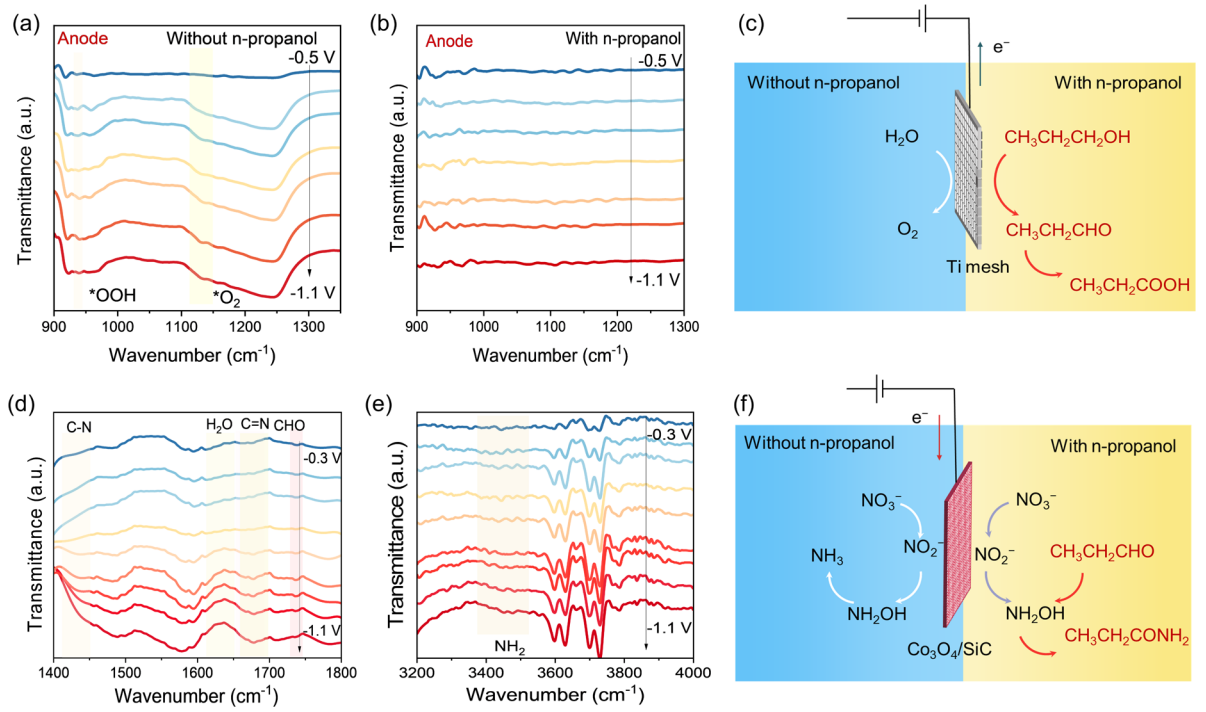

Figure 3. Key reaction intermediates analysis. Potential-dependent in situ FTIR spectra of the electrocatalytic process on the anode side (a) without n-propanol and (b) with n-propanol. (c) The reaction on the anode. (d, e) Potential-dependent in situ FTIR spectra of the electrocatalytic process on the cathode side with n-propanol. (f) The reaction on the cathode.

electrode functioned as the counter and reference electrodes respectively to monitor the reactions occurring at both the cathode (working electrode) and anode (counter electrode) sides during the application of a potential ranging from−0.3 V to−1.1 V vs RHE.

First, the ATR-FTIR spectra before and after the addition of n-propanol were recorded and compared for the anode side (Figure 3a,b). The results demonstrated that in the absence of n-propanol, downward peaks corresponding to *OOH (~942 cm^{-1}) and $*O_2$ (~1129 cm^{-1}) were present, indicating that the OER occurred.[25] The addition of n-propanol, however, suppresses the appearance of these peaks. This observation suggests that the OER is inhibited, but n-propanol oxidation takes place (Figure 3c). Meanwhile, the reaction occurring on the cathode side is also a matter of concern. As evidenced by the presence of NO_2^- and NH_2OH intermediates (Figure S19), nitrate would be reduced to ammonia in the absence of n-propanol. Once the n-propanol was introduced, the NH_2OH signal was nearly absent, however, the presence of NO_2^- remained significant. This suggests that NH_2OH directly participates in the C−N coupling reaction as the intermediate. Moreover, the stretching vibration of C═O (~1750 cm^{-1}) in propionaldehyde, the vibrations of C═N (1677 cm^{-1}) in propionaldehyde oxime and C−N (1438 cm^{-1}) and -NH_2 (3460 cm^{-1}) in propanamide[26−29] are observed in potential-dependent in situ thin-layer FTIR spectra (Figure 3d,e) with the potential ranging from−0.7 to−1.1 V. These findings indicate the presence of intermediates such as propionaldehyde and the formation of the product propionaldehyde oxime and propanamide by the key C−N coupling. Combined with the results from entries 6 and 8 in Table 1 and Figure S15, one can propose that propionaldehyde undergoes a reaction with $*NH_2OH$ intermediates at the cathode(Figure 3f), while NH_2OH does not exhibit reactivity toward propionaldehyde for the formation of propanamide at the anode (entry 9 in Table 1). We consider that the reaction between propionaldehyde and NH_2OH necessitates a cathodic electric field and localized pH conditions.

The reaction path was speculated based on the integration of control experiments, product analysis, in situ characterization, and previous reports,[21] as illustrated in Figure 4. The nitrate on

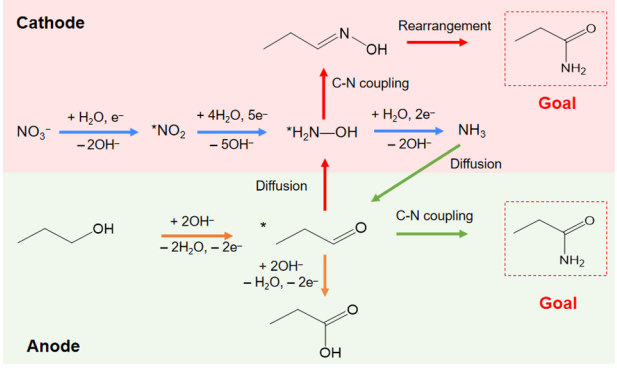

Figure 4. Proposed mechanism. The reaction pathway of cathode−anode coupling to produce propanamide.

the cathode side is initially reduced to intermediates NO_2^- and NH_2OH, while the n-propanol on the anode side undergoes primal oxidation to propionaldehyde intermediates. Next, propionaldehyde reacts with NH_2OH at the cathode to form propionaldehyde oxime, which is then converted into propanamide under the influence of the electric field and localized pH conditions.[21] Specifically, during the nitrate reduction to ammonia at the cathode, protons in water were consumed, generating hydroxide ions and resulting in high local pH. Consequently, the oxime intermediate formed was

https://doi.org/10.1021/jacs.5c01744
J. Am. Chem. Soc. 2025, 147, 16301−16308

dehydrated into nitrile under the action of the electric field and further hydrolyzed into amide due to the locally formed high pH. In the low local pH environment at the anode, the unstable NH_2OH cannot react with aldehyde to form amide, which also verifies this conclusion. The propionaldehyde on the anode side simultaneously undergoes a reaction with the ammonia generated at the cathode and diffused into the electrolyte. We consider that the cathode reaction dominates in these two reactions, as evidenced by the requirement of a higher concentration of NH_3 introduction (1.14 mol/L) than the NO_3RR produced (0.127 mol/L) to form propanamide in entry 8 of Table 1. Further enhancement of the conditional cathode performance and optimization of reaction conditions are anticipated to achieve a higher C−N coupling efficiency.

To achieve a comprehensive understanding of the reaction mechanism of cathode and anode coupling reactions, we conducted density functional theory (DFT) calculations on the Co_3O_4(311) surface of the cathode in Figure 5a and the Ti

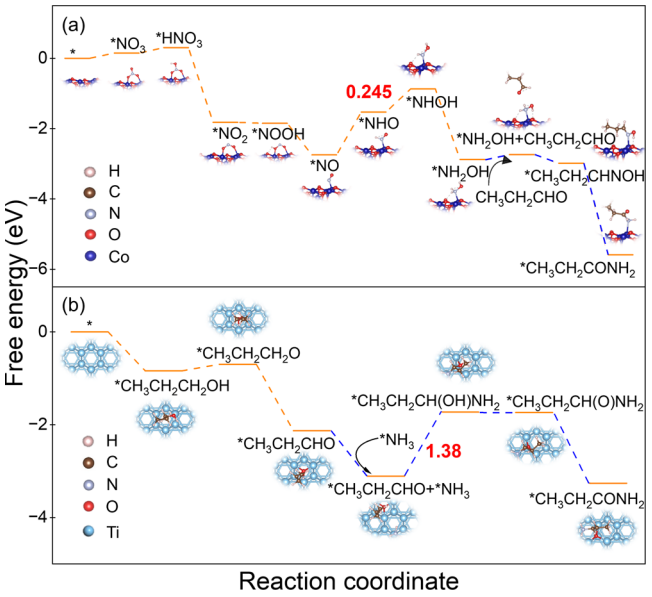

Figure 5. Theoretical calculation for bipolar electrosynthesizing propanamide. The calculated energy profile for (a) cathode and (b) anode reactions, respectively. The electrochemical steps are plotted with orange lines, and nonelectrochemical steps are presented with blue lines.

(111) surface of the anode in Figure 5b. The cathodic reaction includes the electrochemical reaction of NO_3^- to $*NH_2OH$ and the nonelectrochemical reaction of C−N coupling between $*NH_2OH$ and CH_3CH_2CHO to yield propanamide. The crucial step in the cathode reaction involves the conversion of *NO to *NHO, with an energy barrier of 0.25 eV. Simultaneously, the coupling of $*NH_2OH$ and CH_3CH_2CHO to form the critical C−N bond is thermodynamically favorable at the cathode surface (−0.24 eV).

The anode reaction includes the electrochemical reaction of n-propanol to $*CH_3CH_2CHO$, and the nonelectrochemical reaction of NH_3 and $*CH_3CH_2CHO$ to form propanamide. In the anodic reaction for the production of propanamide, n-propanol undergoes oxidation to form propionaldehyde as an intermediate, which is subsequently attacked by nucleophilic ammonia to generate a $*CH_3CH_2CH(OH)NH_2$ intermediate. The participation of this intermediate is crucial in the synthesis of amides. It should be emphasized that ammonia is generated at the cathode via the NO_3RR reaction. The aminopropanol undergoes a dehydrogenation process to yield propanamide, involving two sequential dehydrogenation steps with preferential cleavage of the O−H bond in $*CH_3CH_2CH(OH)NH_2$ over the C−H bond. The generation of intermediate $*CH_3CH_2CH(OH)NH_2$ through the coupling of $*CH_3CH_2CHO$ and NH_3 is identified as the rate-determining step in the anodic production of propanamide, with energy barriers of 1.38 eV. By comparing the energy barriers of the cathodic and anodic reactions, we further validate our hypothesis that the cathodic reaction predominantly contributes to the production of propanamide.

Building upon the foundational research in production efficiency and mechanistic understanding, we conducted a comprehensive technoeconomic analysis (TEA) of the proposed propanamide production strategy at the industrial manufacturing level. This analysis was based on a lately published model (Figure S20 and Notes 1),[30,31] which allowed for a detailed evaluation of the economic viability and sustainability of the process. The results reveal that our anode and cathode synergy coupling electrosynthesis strategy is not only cost-effective but also environmentally sustainable (Figure S21), particularly when factoring in an electricity price of USD 0.03 kWh^{-1}. This analysis highlights the capacity of our approach to optimize resource utilization and reduce environmental impact, reinforcing its potential for scalability and applicability in large-scale industrial settings. The insights gained from this study contribute to the broader discourse on sustainable chemical manufacturing, illustrating how innovative electrochemical methods can align with economic and environmental objectives.

CONCLUSIONS

We developed a new route for the synthesis of propanamide by synergy coupling cathodic nitrate reduction and anodic alcohol oxidation reactions. By modulation of the reaction conditions, propanamide can be produced at a gram scale in the flow cell under ambient conditions. Based on comparative experiments, in situ infrared analysis, and theoretical calculations, a reaction mechanism was proposed. The key reaction intermediates are NH_2OH generated at the cathode and propionaldehyde produced at the anode, which further react at the cathode to synthesize propanamide. This work not only presents a novel avenue for the green synthesis of C−N bonds but also broadens the horizon for electrochemical synthesis of high-value chemicals.

Currently, the bipolar synergy method for synthesizing amides still faces several limitations, notably an imbalance in the electron transfer between the anode and cathode. Specifically, the anode requires eight electrons for ammonia synthesis, whereas the cathode needs only two electrons for aldehyde formation, leading to suboptimal anode utilization. The more compatible anode and cathode reactions could further improve the utilization of the electrosynthesis setup. Additionally, enhancing the performance of nitrate reduction and alcohol oxidation catalysts may facilitate more efficient production of amide products.

ASSOCIATED CONTENT

Supporting Information

The Supporting Information is available free of charge at https://pubs.acs.org/doi/10.1021/jacs.5c01744.

https://doi.org/10.1021/jacs.5c01744
J. Am. Chem. Soc. 2025, 147, 16301−16308

Experimental section; additional electrochemical measurements; material characterizations; and theoretical calculations (PDF)

AUTHOR INFORMATION

Corresponding Authors

Tao Wu − *State Key Laboratory of Fine Chemicals, Liaoning Key Laboratory for Catalytic Conversion of Carbon Resources, School of Chemical Engineering, Dalian University of Technology, Dalian 116024 Liaoning, China;* orcid.org/0000-0001-9543-0377; Email: taowu@dlut.edu.cn

An-Hui Lu − *State Key Laboratory of Fine Chemicals, Liaoning Key Laboratory for Catalytic Conversion of Carbon Resources, School of Chemical Engineering, Dalian University of Technology, Dalian 116024 Liaoning, China;* orcid.org/0000-0003-1294-5928; Email: anhuilu@dlut.edu.cn

Authors

Ming-Hao Guan − *State Key Laboratory of Fine Chemicals, Liaoning Key Laboratory for Catalytic Conversion of Carbon Resources, School of Chemical Engineering, Dalian University of Technology, Dalian 116024 Liaoning, China*

Hao-Nan Xu − *State Key Laboratory of Fine Chemicals, Liaoning Key Laboratory for Catalytic Conversion of Carbon Resources, School of Chemical Engineering, Dalian University of Technology, Dalian 116024 Liaoning, China*

Jin Liu − *State Key Laboratory of Fine Chemicals, Liaoning Key Laboratory for Catalytic Conversion of Carbon Resources, School of Chemical Engineering, Dalian University of Technology, Dalian 116024 Liaoning, China*

Xiao-Ya Zhou − *State Key Laboratory of Fine Chemicals, Liaoning Key Laboratory for Catalytic Conversion of Carbon Resources, School of Chemical Engineering, Dalian University of Technology, Dalian 116024 Liaoning, China*

Complete contact information is available at: https://pubs.acs.org/10.1021/jacs.5c01744

Notes

The authors declare no competing financial interest.

ACKNOWLEDGMENTS

This work was financially supported the Key Program Project of the Joint Fund of National Natural Science Foundation of China (U23A20130) and the Fundamental Research Funds for the Central Universities (DUT22LAB601).

REFERENCES

(1) Shao, J.; Meng, N.; Wang, Y.; Zhang, B.; Yang, K.; Liu, C.; Yu, Y.; Zhang, B. Scalable electrosynthesis of formamide through C−N coupling at the industrially relevant current density of 120 mA cm^{-2}. *Angew. Chem., Int. Ed.* **2022**, *61* (44), No. e202213009.

(2) Jouny, M.; Lv, J.; Cheng, T.; Ko, B.; Zhu, J.; Goddard, W. A., III; Jiao, F. Formation of carbon−nitrogen bonds in carbon monoxide electrolysis. *Nat. Chem.* **2019**, *11* (9), 846−851.

(3) Nagib, D. Nitrogen gets radical. *Nat. Chem.* **2019**, *11* (5), 396−398.

(4) Kilic, B.; Gulcan, H. O.; Aksakal, F.; Ercetin, T.; Oruklu, N.; Bagriacik, E. U.; Dogruer, D. S. Design and synthesis of some new carboxamide and propanamide derivatives bearing phenylpyridazine as a core ring and the investigation of their inhibitory potential on in-vitro acetylcholinesterase and butyrylcholinesterase. *Bioorg. Chem.* **2018**, *79*, 235−249.

(5) He, Y.; He, Y.; Hwang, D.; Ponnusamy, S.; Thiyagarajan, T.; Mohler, M. L.; Narayanan, R.; Miller, D. D. Exploration and biological evaluation of basic heteromonocyclic propanamide derivatives as SARDs for the treatment of enzalutamide-resistant prostate cancer. *J. Med. Chem.* **2021**, *64* (15), 11045−11062.

(6) Massolo, E.; Pirola, M.; Benaglia, M. Amide bond formation strategies: latest advances on a dateless transformation. *Eur. J. Org. Chem.* **2020**, *30*, 4641−4651.

(7) Soyer, Z.; Kılıc, F. S.; Erol, K.; Pabuccuogluet, V. The synthesis and anticonvulsant activity of some ω-phthalimido-N-phenylacetamide and propionamide derivatives. *Arch. Pharm.* **2004**, *337* (2), 105−111.

(8) D'Amaral, M. C.; Jamkhou, N.; Adler, M. J. Efficient and accessible silane-mediated direct amide coupling of carboxylic acids and amines. *Green Chem.* **2021**, *23* (1), 288−295.

(9) El-Faham, A.; Albericio, F. Peptide coupling reagents, more than a letter soup. *Chem. Rev.* **2011**, *111* (11), 6557−6602.

(10) Valeur, E.; Bradley, M. Amide bond formation: beyond the myth of coupling reagents. *Chem. Soc. Rev.* **2009**, *38* (2), 606−631.

(11) Figueiredo, R. M.; Suppo, J.-S.; Campagne, J.-M. Nonclassical routes for amide bond formation. *Chem. Rev.* **2016**, *116* (19), 12029−12122.

(12) Bryan, M. C.; Dunn, P. J.; Entwistle, D.; Gallou, F.; Koenig, S. G.; Hayler, J. D.; Hickey, M. R.; Hughes, S.; Kopach, M. E.; Moine, G.; et al. Key green chemistry research areas from a pharmaceutical manufacturers' perspective revisited. *Green Chem.* **2018**, *20* (22), 5082−5103.

(13) Kingston, C.; Palkowitz, M. D.; Takahira, Y.; Vantourout, J. C.; Peters, B. K.; Kawamata, Y.; Baran, P. S. A survival guide for the "Electro-curious". *Acc. Chem. Res.* **2020**, *53* (1), 72−83.

(14) Jia, S.; Ma, X.; Sun, X.; Han, B. Electrochemical transformation of CO_2 to value-added chemicals and fuels. *CCS Chem.* **2022**, *4* (10), 3213−3229.

(15) Lu, Y.; Li, Y.; Zhou, B.; Wu, J.; Zhou, L.; Pan, Y.; Xia, Z.; Yang, M.; Wu, Y.; Yuan, Z.; et al. Anodic electrosynthesis of amide from alcohol and ammonia. *CCS Chem.* **2024**, *6* (1), 125−136.

(16) Zhou, J.; Han, S.; Yang, R.; Li, T.; Li, W.; Wang, Y.; Yu, Y.; Zhang, B. Linear adsorption enables NO selective electroreduction to hydroxylamine on single Co sites. *Angew. Chem., Int. Ed.* **2023**, *62* (27), No. e202305184.

(17) Tao, Z.; Rooney, C. L.; Liang, Y.; Wang, H. Accessing organonitrogen compounds via C−N coupling in electrocatalytic CO_2 reduction. *J. Am. Chem. Soc.* **2021**, *143* (47), 19630−19642.

(18) Peng, X.; Zeng, L.; Wang, D.; Liu, Z.; Li, Y.; Li, Z.; Yang, B.; Lei, L.; Dai, L.; Hou, Y. Electrochemical C−N coupling of CO_2 and nitrogenous small molecules for the electrosynthesis of organonitrogen compounds. *Chem. Soc. Rev.* **2023**, *52* (6), 2193−2237.

(19) Fu, J.; Yang, Y.; Hu, J.-S. Dual-sites tandem catalysts for C−N bond formation via electrocatalytic coupling of CO_2 and nitrogenous small molecules. *ACS Mater. Lett.* **2021**, *3* (10), 1468−1476.

(20) Kong, X.; Ni, J.; Song, Z.; Yang, Z.; Zheng, J.; Xu, Z.; Qin, L.; Li, H.; Geng, Z.; Zeng, J. Synthesis of hydroxylamine from air and water via a plasma-electrochemical cascade pathway. *Nat. Sustain.* **2024**, *7* (5), 652−660.

(21) Kuang, S.; Xiao, T.; Chi, H.; Liu, J.; Mu, Chao; Liu, H.; Wang, S.; Yu, Y.; Meyer, T. J.; Zhang, S.; et al. Acetamide electrosynthesis from CO_2 and nitrite in water. *Angew. Chem., Int. Ed.* **2024**, *63* (9), No. e202316772.

(22) Li, C.; Wang, Y.; Wang, X.; Azam, T.; Wu, Z.-S. Electrochemical refining of energy-saving coupled systems toward generation of high-value chemicals. *Chem.* **2024**, *10* (9), 2666−2699.

(23) Guan, M.; Xu, H.; Liu, J.; Wu, T.; Lu, A. Strategic regulation of nitrogen-containing intermediates for enhanced nitrate reduction over Co_3O_4/SiC catalyst having multiple active centers. *J.Energy Chem.* **2024**, *96*, 291−299.

(24) Zhou, Z.-Y.; Wang, Q.; Lin, J.-L.; Tian, N.; Sun, S.-G. In situ FTIR spectroscopic studies of electrooxidation of ethanol on Pd electrode in alkaline media. *Electrochim. Acta* **2010**, *55* (27), 7995−7999.

(25) Lin, C.; Li, J.; Li, X.; Yang, S.; Luo, W.; Zhang, Y.; Kim, S.; Kim, D.; Shinde, S. S.; Li, Y.; et al. In-situ reconstructed Ru atom array on α-MnO_2 with enhanced performance for acidic water oxidation. *Nat. Catal.* **2021**, *4* (12), 1012−1023.
(26) Katayama, Y.; Nattino, F.; Giordano, L.; Hwang, J.; Rao, R. R.; Andreussi, O.; Marzari, N.; Yang, S. An in situ surface-enhanced infrared absorption spectroscopy study of electrochemical CO_2 reduction: selectivity dependence on surface C-bound and O-bound reaction intermediates. *J. Phys. Chem. C* **2019**, *123* (10), 5951−5963.
(27) Rodríguez, J. L.; Pastor, E.; Xia, X. H.; Iwasita, T. Reaction intermediates of acetaldehyde oxidation on Pt(111) and Pt(100). *An in situ FTIR study. Langmuir* **2000**, *16* (12), 5479−5486.
(28) Zhu, S.; Jiang, B.; Cai, W. B.; Shao, M. Direct observation on reaction intermediates and the role of bicarbonate anions in CO_2 electrochemical reduction reaction on Cu surfaces. *J. Am. Chem. Soc.* **2017**, *139* (44), 15664−15667.
(29) Guo, C.; Zhou, W.; Lan, X.; Wang, Y.; Li, T.; Han, S.; Yu, Y.; Zhang, B. Electrochemical upgrading of formic acid to formamide via coupling nitrite co-reduction. *J. Am. Chem. Soc.* **2022**, *144* (35), 16006−16011.
(30) Shin, H.; Hansen, K. U.; Jiao, F. Techno-economic assessment of low-temperature carbon dioxide electrolysis. *Nat. Sustain.* **2021**, *4* (10), 911−919.
(31) Jouny, M.; Luc, W.; Jiao, F. General techno-economic analysis of CO_2 electrolysis systems. *Ind. Eng. Chem. Res.* **2018**, *57* (6), 2165−2177.

https://doi.org/10.1021/jacs.5c01744
J. Am. Chem. Soc. 2025, 147, 16301−16308